Evidence for $D^0 - \bar{D}^0$ Mixing Using the CDF II Detector

T. Aaltonen,[23] J. Adelman,[13] T. Akimoto,[54] M. G. Albrow,[17] B. Álvarez González,[11] S. Amerio,[42] D. Amidei,[34]
A. Anastassov,[51] A. Annovi,[19] J. Antos,[14] M. Aoki,[24] G. Apollinari,[17] A. Apresyan,[47] T. Arisawa,[56] A. Artikov,[15]
W. Ashmanskas,[17] A. Attal,[3] A. Aurisano,[52] F. Azfar,[41] P. Azzi-Bacchetta,[42] P. Azzurri,[45] N. Bacchetta,[42] W. Badgett,[17]
A. Barbaro-Galtieri,[28] V. E. Barnes,[47] B. A. Barnett,[25] S. Baroiant,[7] V. Bartsch,[30] G. Bauer,[32] P.-H. Beauchemin,[33]
F. Bedeschi,[45] P. Bednar,[14] S. Behari,[25] G. Bellettini,[45] J. Bellinger,[58] A. Belloni,[22] D. Benjamin,[16] A. Beretvas,[17]
J. Beringer,[28] T. Berry,[29] A. Bhatti,[49] M. Binkley,[17] D. Bisello,[42] I. Bizjak,[30] R. E. Blair,[2] C. Blocker,[6] B. Blumenfeld,[25]
A. Bocci,[16] A. Bodek,[48] V. Boisvert,[48] G. Bolla,[47] A. Bolshov,[32] D. Bortoletto,[47] J. Boudreau,[46] A. Boveia,[10] B. Brau,[10]
A. Bridgeman,[24] L. Brigliadori,[5] C. Bromberg,[35] E. Brubaker,[13] J. Budagov,[15] H. S. Budd,[48] S. Budd,[24] K. Burkett,[17]
G. Busetto,[42] P. Bussey,[21] A. Buzatu,[33] K. L. Byrum,[2] S. Cabrera,[16,s] M. Campanelli,[35] M. Campbell,[34] F. Canelli,[17]
A. Canepa,[44] D. Carlsmith,[58] R. Carosi,[45] S. Carrillo,[18,m] S. Carron,[33] B. Casal,[11] M. Casarsa,[17] A. Castro,[5] P. Catastini,[45]
D. Cauz,[53] M. Cavalli-Sforza,[3] A. Cerri,[28] L. Cerrito,[30,q] S. H. Chang,[27] Y. C. Chen,[1] M. Chertok,[7] G. Chiarelli,[45]
G. Chlachidze,[17] F. Chlebana,[17] K. Cho,[27] D. Chokheli,[15] J. P. Chou,[22] G. Choudalakis,[32] S. H. Chuang,[51] K. Chung,[12]
W. H. Chung,[58] Y. S. Chung,[48] C. I. Ciobanu,[24] M. A. Ciocci,[45] A. Clark,[20] D. Clark,[6] G. Compostella,[42] M. E. Convery,[17]
J. Conway,[7] B. Cooper,[30] K. Copic,[34] M. Cordelli,[19] G. Cortiana,[42] F. Crescioli,[45] C. Cuenca Almenar,[7,s] J. Cuevas,[11,p]
R. Culbertson,[17] J. C. Cully,[34] D. Dagenhart,[17] M. Datta,[17] T. Davies,[21] P. de Barbaro,[48] S. De Cecco,[50] A. Deisher,[28]
G. De Lentdecker,[48,e] G. De Lorenzo,[3] M. Dell'Orso,[45] L. Demortier,[49] J. Deng,[16] M. Deninno,[5] D. De Pedis,[50]
P. F. Derwent,[17] G. P. Di Giovanni,[43] C. Dionisi,[50] B. Di Ruzza,[53] J. R. Dittmann,[4] M. D'Onofrio,[3] S. Donati,[45] P. Dong,[8]
J. Donini,[42] T. Dorigo,[42] S. Dube,[51] J. Efron,[38] R. Erbacher,[7] D. Errede,[24] S. Errede,[24] R. Eusebi,[17] H. C. Fang,[28]
S. Farrington,[29] W. T. Fedorko,[13] R. G. Feild,[59] M. Feindt,[26] J. P. Fernandez,[31] C. Ferrazza,[45] R. Field,[18] G. Flanagan,[47]
R. Forrest,[7] S. Forrester,[7] M. Franklin,[22] J. C. Freeman,[28] I. Furic,[18] M. Gallinaro,[49] J. Galyardt,[12] F. Garberson,[10]
J. E. Garcia,[45] A. F. Garfinkel,[47] H. Gerberich,[24] D. Gerdes,[34] S. Giagu,[50] V. Giakoumopoulou,[45,b] P. Giannetti,[45]
K. Gibson,[46] J. L. Gimmell,[48] C. M. Ginsburg,[17] N. Giokaris,[15,b] M. Giordani,[53] P. Giromini,[19] M. Giunta,[45] V. Glagolev,[15]
D. Glenzinski,[17] M. Gold,[36] N. Goldschmidt,[18] A. Golossanov,[17] G. Gomez,[11] G. Gomez-Ceballos,[32] M. Goncharov,[52]
O. González,[31] I. Gorelov,[36] A. T. Goshaw,[16] K. Goulianos,[49] A. Gresele,[42] S. Grinstein,[22] C. Grosso-Pilcher,[13]
R. C. Group,[17] U. Grundler,[24] J. Guimaraes da Costa,[22] Z. Gunay-Unalan,[35] C. Haber,[28] K. Hahn,[32] S. R. Hahn,[17]
E. Halkiadakis,[51] A. Hamilton,[20] B.-Y. Han,[48] J. Y. Han,[48] R. Handler,[58] F. Happacher,[19] K. Hara,[54] D. Hare,[51] M. Hare,[55]
S. Harper,[41] R. F. Harr,[57] R. M. Harris,[17] M. Hartz,[46] K. Hatakeyama,[49] J. Hauser,[8] C. Hays,[41] M. Heck,[26] A. Heijboer,[44]
B. Heinemann,[28] J. Heinrich,[44] C. Henderson,[32] M. Herndon,[58] J. Heuser,[26] S. Hewamanage,[4] D. Hidas,[16] C. S. Hill,[10,d]
D. Hirschbuehl,[26] A. Hocker,[17] S. Hou,[1] M. Houlden,[29] S.-C. Hsu,[9] B. T. Huffman,[41] R. E. Hughes,[38] U. Husemann,[59]
J. Huston,[35] J. Incandela,[10] G. Introzzi,[45] M. Iori,[50] A. Ivanov,[7] B. Iyutin,[32] E. James,[17] B. Jayatilaka,[16] D. Jeans,[50]
E. J. Jeon,[27] S. Jindariani,[18] W. Johnson,[7] M. Jones,[47] K. K. Joo,[27] S. Y. Jun,[12] J. E. Jung,[27] T. R. Junk,[24] T. Kamon,[52]
D. Kar,[18] P. E. Karchin,[57] Y. Kato,[40] R. Kephart,[17] U. Kerzel,[26] V. Khotilovich,[52] B. Kilminster,[38] D. H. Kim,[27]
H. S. Kim,[27] J. E. Kim,[27] M. J. Kim,[17] S. B. Kim,[27] S. H. Kim,[54] Y. K. Kim,[13] N. Kimura,[54] L. Kirsch,[6] S. Klimenko,[18]
M. Klute,[32] B. Knuteson,[32] B. R. Ko,[16] S. A. Koay,[10] K. Kondo,[56] D. J. Kong,[27] J. Konigsberg,[18] A. Korytov,[18]
A. V. Kotwal,[16] J. Kraus,[24] M. Kreps,[26] J. Kroll,[44] N. Krumnack,[4] M. Kruse,[16] V. Krutelyov,[10] T. Kubo,[54] S. E. Kuhlmann,[2]
T. Kuhr,[26] N. P. Kulkarni,[57] Y. Kusakabe,[56] S. Kwang,[13] A. T. Laasanen,[47] S. Lai,[33] S. Lami,[45] S. Lammel,[17]
M. Lancaster,[30] R. L. Lander,[7] K. Lannon,[38] A. Lath,[51] G. Latino,[45] I. Lazzizzera,[42] T. LeCompte,[2] J. Lee,[48] J. Lee,[27]
Y. J. Lee,[27] S. W. Lee,[52,r] R. Lefèvre,[20] N. Leonardo,[32] S. Leone,[45] S. Levy,[13] J. D. Lewis,[17] C. Lin,[59] C. S. Lin,[28]
J. Linacre,[41] M. Lindgren,[17] E. Lipeles,[9] A. Lister,[7] D. O. Litvintsev,[17] T. Liu,[17] N. S. Lockyer,[44] A. Loginov,[59] M. Loreti,[42]
L. Lovas,[14] R.-S. Lu,[1] D. Lucchesi,[42] J. Lueck,[26] C. Luci,[50] P. Lujan,[28] P. Lukens,[17] G. Lungu,[18] L. Lyons,[41] J. Lys,[28]
R. Lysak,[14] E. Lytken,[47] P. Mack,[26] D. MacQueen,[33] R. Madrak,[17] K. Maeshima,[17] K. Makhoul,[32] T. Maki,[23]
P. Maksimovic,[25] S. Malde,[41] S. Malik,[30] G. Manca,[29] A. Manousakis,[15,b] F. Margaroli,[47] C. Marino,[26] C. P. Marino,[24]
A. Martin,[59] M. Martin,[25] V. Martin,[21,k] M. Martínez,[3] R. Martínez-Ballarín,[31] T. Maruyama,[54] P. Mastrandrea,[50]
T. Masubuchi,[54] M. E. Mattson,[57] P. Mazzanti,[5] K. S. McFarland,[48] P. McIntyre,[52] R. McNulty,[29,j] A. Mehta,[29]
P. Mehtala,[23] S. Menzemer,[11,l] A. Menzione,[45] P. Merkel,[47] C. Mesropian,[49] A. Messina,[35] T. Miao,[17] N. Miladinovic,[6]
J. Miles,[32] R. Miller,[35] C. Mills,[22] M. Milnik,[26] A. Mitra,[1] G. Mitselmakher,[18] H. Miyake,[54] S. Moed,[22] N. Moggi,[5]
C. S. Moon,[27] R. Moore,[17] M. Morello,[45] P. Movilla Fernandez,[28] J. Mülmenstädt,[28] A. Mukherjee,[17] Th. Muller,[26]
R. Mumford,[25] P. Murat,[17] M. Mussini,[5] J. Nachtman,[17] Y. Nagai,[54] A. Nagano,[54] J. Naganoma,[56] K. Nakamura,[54]

121802-1

I. Nakano,[39] A. Napier,[55] V. Necula,[16] C. Neu,[44] M. S. Neubauer,[24] J. Nielsen,[28,g] L. Nodulman,[2] M. Norman,[9]
O. Norniella,[24] E. Nurse,[30] S. H. Oh,[16] Y. D. Oh,[27] I. Oksuzian,[18] T. Okusawa,[40] R. Oldeman,[29] R. Orava,[23] K. Osterberg,[23]
S. Pagan Griso,[42] C. Pagliarone,[45] E. Palencia,[17] V. Papadimitriou,[17] A. Papaikonomou,[26] A. A. Paramonov,[13] B. Parks,[38]
S. Pashapour,[33] J. Patrick,[17] G. Pauletta,[53] M. Paulini,[12] C. Paus,[32] D. E. Pellett,[7] A. Penzo,[53] T. J. Phillips,[16]
G. Piacentino,[45] J. Piedra,[43] L. Pinera,[18] K. Pitts,[24] C. Plager,[8] L. Pondrom,[58] X. Portell,[3] O. Poukhov,[15] N. Pounder,[41]
F. Prakoshyn,[15] A. Pronko,[17] J. Proudfoot,[2] F. Ptohos,[17,i] G. Punzi,[45] J. Pursley,[58] J. Rademacker,[41,d] A. Rahaman,[46]
V. Ramakrishnan,[58] N. Ranjan,[47] I. Redondo,[31] B. Reisert,[17] V. Rekovic,[36] P. Renton,[41] M. Rescigno,[50] S. Richter,[26]
F. Rimondi,[5] L. Ristori,[45] A. Robson,[21] T. Rodrigo,[11] E. Rogers,[24] S. Rolli,[55] R. Roser,[17] M. Rossi,[53] R. Rossin,[10] P. Roy,[33]
A. Ruiz,[11] J. Russ,[12] V. Rusu,[17] H. Saarikko,[23] A. Safonov,[52] W. K. Sakumoto,[48] G. Salamanna,[50] O. Saltó,[3] L. Santi,[53]
S. Sarkar,[50] L. Sartori,[45] K. Sato,[17] A. Savoy-Navarro,[43] T. Scheidle,[26] P. Schlabach,[17] E. E. Schmidt,[17] M. A. Schmidt,[13]
M. P. Schmidt,[59] M. Schmitt,[37] T. Schwarz,[7] L. Scodellaro,[11] A. L. Scott,[10] A. Scribano,[45] F. Scuri,[45] A. Sedov,[47]
S. Seidel,[36] Y. Seiya,[40] A. Semenov,[15] L. Sexton-Kennedy,[17] A. Sfyria,[20] S. Z. Shalhout,[57] M. D. Shapiro,[28] T. Shears,[29]
P. F. Shepard,[46] D. Sherman,[22] M. Shimojima,[54,o] M. Shochet,[13] Y. Shon,[58] I. Shreyber,[20] A. Sidoti,[45] P. Sinervo,[33]
A. Sisakyan,[15] A. J. Slaughter,[17] J. Slaunwhite,[38] K. Sliwa,[55] J. R. Smith,[7] F. D. Snider,[17] R. Snihur,[33] M. Soderberg,[34]
A. Soha,[7] S. Somalwar,[51] V. Sorin,[35] J. Spalding,[17] F. Spinella,[45] T. Spreitzer,[33] P. Squillacioti,[45] M. Stanitzki,[59]
R. St. Denis,[21] B. Stelzer,[8] O. Stelzer-Chilton,[41] D. Stentz,[37] J. Strologas,[36] D. Stuart,[10] J. S. Suh,[27] A. Sukhanov,[18]
H. Sun,[55] I. Suslov,[15] T. Suzuki,[54] A. Taffard,[24,f] R. Takashima,[39] Y. Takeuchi,[54] R. Tanaka,[39] M. Tecchio,[34] P. K. Teng,[1]
K. Terashi,[49] J. Thom,[17,h] A. S. Thompson,[21] G. A. Thompson,[24] E. Thomson,[44] P. Tipton,[59] V. Tiwari,[12] S. Tkaczyk,[17]
D. Toback,[52] S. Tokar,[14] K. Tollefson,[35] T. Tomura,[54] D. Tonelli,[17] S. Torre,[19] D. Torretta,[17] S. Tourneur,[43] W. Trischuk,[33]
Y. Tu,[44] N. Turini,[45] F. Ukegawa,[54] S. Uozumi,[54] S. Vallecorsa,[20] N. van Remortel,[23] A. Varganov,[34] E. Vataga,[36]
F. Vázquez,[18,m] G. Velev,[17] C. Vellidis,[45,b] V. Veszpremi,[47] M. Vidal,[31] R. Vidal,[17] I. Vila,[11] R. Vilar,[11] T. Vine,[30]
M. Vogel,[36] I. Volobouev,[28,r] G. Volpi,[45] F. Würthwein,[9] P. Wagner,[44] R. G. Wagner,[2] R. L. Wagner,[17] J. Wagner-Kuhr,[26]
W. Wagner,[26] T. Wakisaka,[40] R. Wallny,[8] S. M. Wang,[1] A. Warburton,[33] D. Waters,[30] M. Weinberger,[52] W. C. Wester III,[17]
B. Whitehouse,[55] D. Whiteson,[44,f] A. B. Wicklund,[2] E. Wicklund,[17] G. Williams,[33] H. H. Williams,[44] P. Wilson,[17]
B. L. Winer,[38] P. Wittich,[17,h] S. Wolbers,[17] C. Wolfe,[13] T. Wright,[34] X. Wu,[20] S. M. Wynne,[29] A. Yagil,[9] K. Yamamoto,[40]
J. Yamaoka,[51] T. Yamashita,[39] C. Yang,[59] U. K. Yang,[13,n] Y. C. Yang,[27] W. M. Yao,[28] G. P. Yeh,[17] J. Yoh,[17] K. Yorita,[13]
T. Yoshida,[40] G. B. Yu,[48] I. Yu,[27] S. S. Yu,[17] J. C. Yun,[17] L. Zanello,[50] A. Zanetti,[53] I. Zaw,[22] X. Zhang,[24]
Y. Zheng,[8,c] and S. Zucchelli[5]

(CDF Collaboration)[a]

[1]*Institute of Physics, Academia Sinica, Taipei, Taiwan 11529, Republic of China*
[2]*Argonne National Laboratory, Argonne, Illinois 60439, USA*
[3]*Institut de Fisica d'Altes Energies, Universitat Autonoma de Barcelona, E-08193, Bellaterra (Barcelona), Spain*
[4]*Baylor University, Waco, Texas 76798, USA*
[5]*Istituto Nazionale di Fisica Nucleare, University of Bologna, I-40127 Bologna, Italy*
[6]*Brandeis University, Waltham, Massachusetts 02254, USA*
[7]*University of California, Davis, Davis, California 95616, USA*
[8]*University of California, Los Angeles, Los Angeles, California 90024, USA*
[9]*University of California, San Diego, La Jolla, California 92093, USA*
[10]*University of California, Santa Barbara, Santa Barbara, California 93106, USA*
[11]*Instituto de Fisica de Cantabria, CSIC–University of Cantabria, 39005 Santander, Spain*
[12]*Carnegie Mellon University, Pittsburgh, Pennsylvania 15213, USA*
[13]*Enrico Fermi Institute, University of Chicago, Chicago, Illinois 60637, USA*
[14]*Comenius University, 842 48 Bratislava, Slovakia; Institute of Experimental Physics, 040 01 Kosice, Slovakia*
[15]*Joint Institute for Nuclear Research, RU-141980 Dubna, Russia*
[16]*Duke University, Durham, North Carolina 27708*
[17]*Fermi National Accelerator Laboratory, Batavia, Illinois 60510, USA*
[18]*University of Florida, Gainesville, Florida 32611, USA*
[19]*Laboratori Nazionali di Frascati, Istituto Nazionale di Fisica Nucleare, I-00044 Frascati, Italy*
[20]*University of Geneva, CH-1211 Geneva 4, Switzerland*
[21]*Glasgow University, Glasgow G12 8QQ, United Kingdom*
[22]*Harvard University, Cambridge, Massachusetts 02138, USA*
[23]*Division of High Energy Physics, Department of Physics, University of Helsinki and Helsinki Institute of Physics,
FIN-00014, Helsinki, Finland*

^{24}University of Illinois, Urbana, Illinois 61801, USA

^{25}The Johns Hopkins University, Baltimore, Maryland 21218, USA

^{26}Institut für Experimentelle Kernphysik, Universität Karlsruhe, 76128 Karlsruhe, Germany

^{27}Center for High Energy Physics: Kyungpook National University, Daegu 702-701, Korea;

Seoul National University, Seoul 151-742, Korea;

Sungkyunkwan University, Suwon 440-746, Korea;

Korea Institute of Science and Technology Information, Daejeon, 305-806, Korea;

Chonnam National University, Gwangju, 500-757, Korea

^{28}Ernest Orlando Lawrence Berkeley National Laboratory, Berkeley, California 94720, USA

^{29}University of Liverpool, Liverpool L69 7ZE, United Kingdom

^{30}University College London, London WC1E 6BT, United Kingdom

^{31}Centro de Investigaciones Energeticas Medioambientales y Tecnologicas, E-28040 Madrid, Spain

^{32}Massachusetts Institute of Technology, Cambridge, Massachusetts 02139, USA

^{33}Institute of Particle Physics: McGill University, Montréal, Canada H3A 2T8;

and University of Toronto, Toronto, Canada M5S 1A7

^{34}University of Michigan, Ann Arbor, Michigan 48109, USA

^{35}Michigan State University, East Lansing, Michigan 48824, USA

^{36}University of New Mexico, Albuquerque, New Mexico 87131, USA

^{37}Northwestern University, Evanston, Illinois 60208, USA

^{38}The Ohio State University, Columbus, Ohio 43210, USA

^{39}Okayama University, Okayama 700-8530, Japan

^{40}Osaka City University, Osaka 588, Japan

^{41}University of Oxford, Oxford OX1 3RH, United Kingdom

^{42}University of Padova, Istituto Nazionale di Fisica Nucleare, Sezione di Padova-Trento, I-35131 Padova, Italy

^{43}LPNHE, Universite Pierre et Marie Curie/IN2P3-CNRS, UMR7585, Paris, F-75252 France

^{44}University of Pennsylvania, Philadelphia, Pennsylvania 19104, USA

^{45}Istituto Nazionale di Fisica Nucleare Pisa, Universities of Pisa, Siena and Scuola Normale Superiore, I-56127 Pisa, Italy

^{46}University of Pittsburgh, Pittsburgh, Pennsylvania 15260, USA

^{47}Purdue University, West Lafayette, Indiana 47907, USA

^{48}University of Rochester, Rochester, New York 14627, USA

^{49}The Rockefeller University, New York, New York 10021, USA

^{50}Istituto Nazionale di Fisica Nucleare, Sezione di Roma 1, University of Rome "La Sapienza," I-00185 Roma, Italy

^{51}Rutgers University, Piscataway, New Jersey 08855, USA

^{52}Texas A&M University, College Station, Texas 77843, USA

^{53}Istituto Nazionale di Fisica Nucleare, University of Trieste/Udine, Italy

^{54}University of Tsukuba, Tsukuba, Ibaraki 305, Japan

^{55}Tufts University, Medford, Massachusetts 02155, USA

^{56}Waseda University, Tokyo 169, Japan

^{57}Wayne State University, Detroit, Michigan 48201, USA

^{58}University of Wisconsin, Madison, Wisconsin 53706, USA

^{59}Yale University, New Haven, Connecticut 06520, USA

We measure the time dependence of the ratio of decay rates for the rare decay $D^0 \rightarrow K^+ \pi^-$ to the Cabibbo-favored decay $D^0 \rightarrow K^- \pi^+$. A signal of 12.7×10^3 $D^0 \rightarrow K^+ \pi^-$ decays was obtained using the Collider Detector at Fermilab II detector at the Fermilab Tevatron with an integrated luminosity of 1.5 fb^{-1}. We measure the $D^0 - \bar{D}^0$ mixing parameters (R_D, y', x'^2), and find that the data are inconsistent with the no-mixing hypothesis with a probability equivalent to 3.8 Gaussian standard deviations.

Since the discovery of the charm quark in 1974 [1,2], physicists have been searching for the oscillation of neutral charm mesons between particle and antiparticle states. Such behavior is referred to as ''mixing,'' as first explained in 1955 [3] for the K^0 meson in terms of quantum-mechanical mixed states. Mixing was next studied for B^0 mesons in 1987 [4,5]. The years 2006 and 2007 have seen landmark new results on mixing: first time-dependent observation of B_s mixing from the CDF experiment [6] and

evidence for D^0 mixing from the *BABAR* [7] and Belle [8] experiments.

The recent evidence for D^0 mixing comes from two different types of measurements. The Belle Collaboration found direct evidence for a longer and shorter lived D^0 meson, in analogy to the well-known case for K^0 mesons. They found significantly different decay time distributions for D^0 decays to the *CP* eigenstates $K^+ K^-$ and $\pi^+ \pi^-$ compared to that for the *CP*-mixed state $K^- \pi^+$. (In this

Letter, reference to a specific decay chain implicitly includes the charge-conjugate decay.) No other experiment has confirmed the evidence for lifetime differences among these decays [9]. The evidence for D^0 mixing found in the *BABAR* experiment is a difference in decay time distribution for $D^0 \to K^+ \pi^-$ compared to that for the Cabibbo-favored (CF) decay $D^0 \to K^- \pi^+$. This same measurement was made in the Belle experiment [10], but evidence for mixing was not seen. In this Letter, we present a new measurement of the same D^0 mixing process as used by *BABAR* for their evidence.

In the standard model, the decay $D^0 \to K^+ \pi^-$ proceeds through a doubly Cabibbo-suppressed (DCS) "tree" diagram, and may also result from a mixing process ($D^0 \leftrightarrow \bar{D}^0$), if it exists, followed by a CF decay ($\bar{D}^0 \to K^+ \pi^-$). The DCS decay rate depends on Cabibbo-Kobayashi-Maskawa quark-mixing matrix elements and on the magnitude of SU(3) flavor symmetry violation [11]. Mixing may occur through two distinct types of second-order weak processes. In "long-range" mixing, the D^0 evolves into a virtual hadronic state such as $\pi^+ \pi^-$, which subsequently evolves to a $\bar{D}^0$. The amplitude for long-range mixing has been estimated using strong interaction models [12], but has not been determined using a QCD calculation from first principles. "Short-range" processes [13] have a "box" or "penguin" topology, and are negligible in the standard model. However, exotic weakly interacting particles could enhance the short-range mixing and provide a signature of new physics [14–16].

The ratio R of $D^0 \to K^+ \pi^-$ to $D^0 \to K^- \pi^+$ decay rates can be approximated [17,18] as a simple quadratic function of t/τ, where t is the proper decay time and τ is the mean D^0 lifetime. This form is valid assuming *CP* conservation and small values for the parameters $x = \Delta M/\Gamma$ and $y = \Delta\Gamma/2\Gamma$, where ΔM is the mass difference between the D^0 meson weak eigenstates, $\Delta\Gamma$ is the decay width difference, and Γ is the average decay width of the eigenstates. Under the assumptions stated above,

$$R(t/\tau) = R_D + \sqrt{R_D}\, y'(t/\tau) + \frac{x'^2 + y'^2}{4}(t/\tau)^2, \quad (1)$$

where R_D is the squared modulus of the ratio of DCS to CF amplitudes, $x' = x\cos\delta + y\sin\delta$, $y' = -x\sin\delta + y\cos\delta$, and δ is the strong interaction phase difference between the DCS and CF amplitudes. In the absence of mixing, $x' = y' = 0$ and $R(t/\tau) = R_D$.

Our measurement uses data collected by the CDF II detector at the Fermilab Tevatron collider, from February 2002 to January 2007, corresponding to an integrated luminosity of ≈ 1.5 fb^{-1} for $p\bar{p}$ collisions at $\sqrt{s} = 1.96$ TeV. CDF II [19] is a multipurpose detector with a magnetic spectrometer surrounded by a calorimeter and a muon detector. The detector components pertinent to this analysis are the silicon microstrip vertex detector, the multiwire drift chamber (COT), and the 1.4 T magnet,

which together measure the trajectories and momenta of charged particles. The COT measures ionization energy loss for a charged particle, which is used for particle identification (PID).

Events are selected in real time with a trigger system developed for a broad class of heavy flavor decays. The trigger requirements used here are the same as those described for our previous measurement of the time-integrated value of R [20], which used a smaller data sample. The trigger selects events with a pair of oppositely charged particles that are consistent with originating from a secondary decay vertex separated from the beam line.

In the off-line analysis, we reconstruct the "right-sign" (RS) CF decay chain $D^{*+} \to \pi^+ D^0$, $D^0 \to K^- \pi^+$, and the "wrong-sign" (WS) decay chain $D^{*+} \to \pi^+ D^0$, $D^0 \to K^+ \pi^-$. The relative charges of the pions determine whether the decay chain is RS (like charge) or WS (opposite charge). The reconstruction method is similar to that used for our previous time-independent measurement. Since the RS and WS D^* decays have the same kinematics, we use the same selection criteria (cuts) for both the RS and WS decay modes to reduce systematic uncertainties. Analysis cuts were optimized before the WS candidates were revealed.

The D^0 candidate reconstruction starts with a pair of tracks from oppositely charged particles that satisfy the trigger requirements. The tracks are considered with both $K^- \pi^+$ and $\pi^- K^+$ interpretations. A third "tagging" track, required to have $p_T \geq 0.3$ GeV/c, is used to form a D^* candidate when considered as a pion and combined with the D^0 candidate.

We apply two cuts to the WS signal to reduce the background from RS decays where the D^0 decay tracks are misidentified because the kaon and pion assignments are mistakenly interchanged. As determined from the data, 96.4% of D^0 decays with correct mass assignment are reconstructed with $K\pi$ invariant mass $m_{K\pi}$ within 20 MeV/c^2 of the D^0 mass. The $m_{K\pi}$ distribution for misidentified D^0 decays is much broader, and has only 22% of the events within the same mass range. We remove WS candidates that have a RS mass within that range. This cut excludes 96.4% of RS decays and retains 78% of the WS signal. We also impose a cut based on PID, which is used to distinguish pions from kaons for all three tracks in the decay chain. This cut, described in Ref. [20], further helps to reject misidentified decays.

We use a series of cuts based on the decay topology of signal events in which a D^* and its tagging pion are produced at the primary vertex, and the D^0 travels a measurable distance before decay. The cuts reduce background from combinations with one or more tracks not from the D^* decay. We require the transverse decay length significance L_{xy}/σ_{xy} to be greater than 4, where $L_{xy} = \vec{r} \cdot \vec{p}_T/p_T$, $\vec{r}$ is the distance between the primary and D^0 decay vertices, $\vec{p}_T$ is the transverse component of the
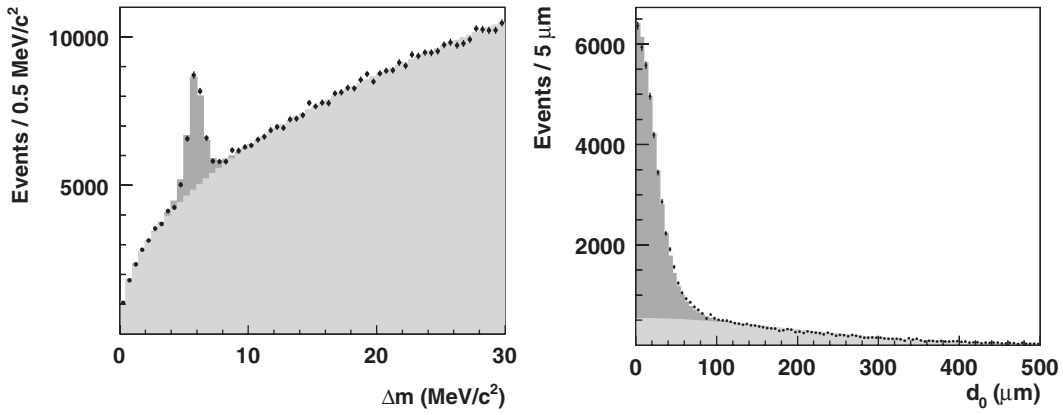
FIG. 1.   (left) Time-integrated distribution for "wrong-sign" $D^0 \to K^+ \pi^-$ signal yield as a function of Δm. Also shown is the result of a least-squares fit using an empirical function for the signal (dark shaded region) and a power law for the background (light shaded region). (right) Distribution of transverse impact parameter d_0 for D^0 mesons with $5 < t/\tau < 6$ for "right-sign" D^* mesons. The result of a binned maximum likelihood fit shows the narrow peak due to promptly produced D^* mesons (dark shaded) and the broad distribution due to nonprompt D^* mesons from B decay (light shaded).

momentum of the D^0 candidate with respect to the beam line, and σ_{xy} is the uncertainty on L_{xy}. The tagging pion track must have $d_0 < 500$ μm, where the transverse impact parameter d_0 is the distance of closest approach between a track and the primary vertex in the plane transverse to the beam line. The tagging pion must also have a point of closest approach to the primary vertex less than 1.5 cm along the beam line.

The ratio t/τ is determined for each D^0 candidate by $t/\tau = m_{D^0} L_{xy}/(p_T \tau)$, where $m_{D^0} = 1.8648$ GeV/c^2 and $\tau = 410.1$ fs are the world average values for the D^0 invariant mass and lifetime, respectively [21]. To study $R(t/\tau)$, we divide the data into 20 bins of t/τ ranging from 0.75 to 10.0, choosing bins of increasing size from

0.25 to 2.0 to reduce statistical uncertainty at larger times. The bin sizes are larger than the t/τ resolution of ≈ 0.16.

After RS and WS candidates are separately divided into t/τ bins, they are further divided into bins of mass difference $\Delta m \equiv m_{K\pi\pi} - m_{K\pi} - m_{\pi}$. For each Δm bin, we perform a binned maximum likelihood fit of the corresponding $m_{K\pi}$ distribution to determine the D^0 signal yield. The distribution of D^0 signal yield versus Δm is fit using a least-squares method to get the D^* signal for each time bin. The D^* fit procedure is illustrated by the time-integrated WS Δm distribution shown in Fig. 1 (left).

The signal shapes for the $m_{K\pi}$ and Δm distributions are fixed from the RS time-integrated fits. For each $m_{K\pi}$ distribution, a parabola with floating parameters is used
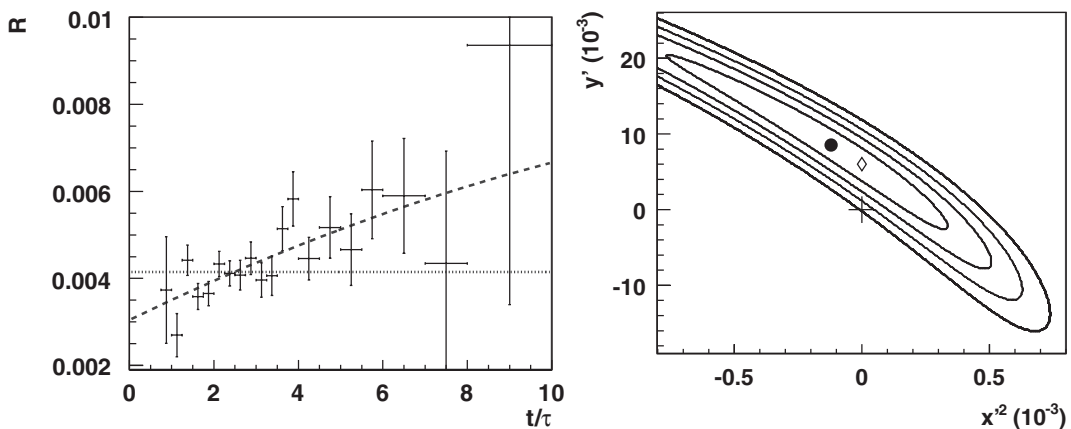

FIG. 2.   (left) Ratio of prompt D^* "wrong-sign" to "right-sign" decays as a function of normalized proper decay time. The dashed curve is from a least-squares parabolic fit, which determines the parameters R_D, y', and x'^2. The dotted line is the fit assuming no mixing. (right) Bayesian probability contours in the $x'^2 - y'$ parameter space corresponding to one through four equivalent Gaussian standard deviations. The closed circle shows the unconstrained fit values for the mixing parameters. The open diamond shows the values from the physically allowed fit ($x'^2 \geq 0$). The cross shows the no-mixing point.

to fit the background. The background shapes for all the Δm WS (RS) distributions are fixed to the shape determined for the time-integrated WS (RS) distribution. The amplitudes of the signal and background shapes are determined independently for all $m_{K\pi}$ and Δm fits. The RS distributions have similar amounts of background as the WS distributions, but the RS signal is about 250 times larger.

The D^* mesons that originate from beauty hadron (B) decays must be treated as background to avoid the complication of measuring the D^0 decay length from the B decay point instead of the primary vertex. The D^* mesons produced promptly at the primary vertex have a narrow d_0 distribution for their daughter D^0 mesons, with a shape independent of t/τ. The background from nonprompt D^* mesons from the decay chain $B \rightarrow D^* \rightarrow D^0$ have a broad d_0 distribution, due to the decay length of the B hadrons. The width of the broad distribution increases with increasing t/τ. An example d_0 distribution is shown in Fig. 1 (right). The shapes of the prompt and broad distributions are determined from RS data. The WS shapes are the same as the RS shapes. For each of the 20 t/τ bins, the prompt WS (RS) signal is determined from the number of WS (RS) D^* mesons and the shapes of the d_0 distributions. The ratio of nonprompt to prompt signal is ≈ 0.02 at $t/\tau = 2$ and increases with increasing t/τ due to the faster exponential falloff with t/τ for D^0 compared to B. At $t/\tau = 7$, the ratio is ≈ 1.

The time-integrated prompt D^* signals are $(12.7 \pm 0.3) \times 10^3$ WS events and $(3.044 \pm 0.002) \times 10^6$ RS events. The ratios of prompt WS to RS signal for the 20 t/τ bins are shown in Fig. 2 (left). The uncertainties for each bin include statistical and systematic contributions. The significant systematic uncertainties are due to the background shapes for the $m_{K\pi}$, Δm, and d_0 distributions, which are described by parameters that are allowed to vary in the fitting procedure. We used simulation to confirm that our choice of decay time bins does not systematically affect the result. The detector acceptances for RS and WS decays are nearly identical, and their difference contributes a negligible systematic uncertainty in the ratio R. The bins at small and large t/τ with larger uncertainties are due to smaller numbers of signal events, due to the trigger turn-on and exponential decay rate, respectively.

A least-squares parabolic fit of the data in Fig. 2 (left) to Eq. (1) determines the values and uncertainties for the parameters R_D, y', and x'^2, which are listed in Table I. Since the value of x'^2 is unphysical (less than zero), but consistent with zero, we also fit the data with the constraint $x'^2 = 0$. The values of R_D and y' are consistent with and without the constraint. The values and precision of the parameters measured by CDF are comparable to those from the best previous measurements, as shown in Table II.

To determine the consistency of our data with the no-mixing hypothesis, we compute Bayesian contours containing the region with the highest posterior probability. The probability density is calculated as the product of a likelihood $\mathcal{L}$ and a prior, divided by a normalization factor. The likelihood is $\mathcal{L} = \exp(-\chi^2/2)$, where χ^2 is computed from the data in Fig. 2 (left) for a particular set of fit parameters. A flat prior is used for all three parameters, and R_D is treated as a Bayesian nuisance parameter. The contours are insensitive to modest changes in the prior. The contours in the x'^2-y' plane are shown in Fig. 2 (right). The no-mixing point lies on the contour, which excludes a region containing a probability of 1.5×10^{-4}, equivalent to 3.8 Gaussian standard deviations. We also computed contours with the constraint $x'^2 \geq 0$ and find a probability for no-mixing consistent with the value obtained without the constraint.

We tried alternate procedures to determine the probability for no mixing. We fit the data in Fig. 2 (left) with the constraint $y' = x'^2 = 0$, with results as given in Table I. The change in log likelihood ($-2\Delta \ln \mathcal{L}$) between the unconstrained and no-mixing fits has an approximately chi-square distribution for 2 degrees of freedom. From Table I, $-2\Delta \ln \mathcal{L} = 17.6$, which corresponds to a probability of 1.6×10^{-4}. We also made a frequentist check using ensembles of simulated $R(t/\tau)$ measurements without mixing. The probability for a simulation to have a value of $-2\Delta \ln \mathcal{L} \geq 17.6$ is 1.3×10^{-4}. The probabilities from both of these checks are consistent with that obtained using Bayesian contours.

In conclusion, our data show evidence for $D^0 - \bar{D}^0$ mixing in the $K^+\pi^-$ channel, providing the first confirmation of the evidence in this channel from the *BABAR* experiment. The mixing could be due to standard model long-range intermediate states or due to new physics. Improved reliability of standard model calculations and

TABLE I. Fit results for the $R(t/\tau)$ distribution. The uncertainties include statistical and systematic components. The correlation coefficient between y' and x'^2 for the unconstrained fit is -0.98. The no-mixing fit is consistent with our previous time-independent result [20].

Fit type	$R_D(10^{-3})$	$y'(10^{-3})$	$x'^2(10^{-3})$	χ^2/d.o.f.
Unconstrained	3.04 ± 0.55	8.5 ± 7.6	-0.12 ± 0.35	19.2/17
Physically allowed	3.22 ± 0.23	6.0 ± 1.4	0	19.3/18
No mixing	4.15 ± 0.10	0	0	36.8/19

TABLE II.   Comparison of the CDF result with recent measurements. All results use $D^0 \rightarrow K^+\pi^-$ decays and fits assuming no CP violation. The uncertainties include statistical and systematic components. The significance for no mixing is given in terms of the equivalent number of Gaussian standard deviations.

Experiment	$R_D(10^{-3})$	$y'(10^{-3})$	$x'^2(10^{-3})$	Mixing Signif.
CDF	3.04 ± 0.55	8.5 ± 7.6	-0.12 ± 0.35	3.8
BABAR [7]	3.03 ± 0.19	9.7 ± 5.4	-0.22 ± 0.37	3.9
Belle [10]	3.64 ± 0.17	$0.6 + 4.0 - 3.9$	$0.18 + 0.21 - 0.23$	2.0

future measurements of mixing signatures with improved precision are needed to explain this phenomenon.

[a]With visitors from:

[b]University of Athens, 15784 Athens, Greece.

[c]Chinese Academy of Sciences, Beijing 100864, China.

[d]University of Bristol, Bristol BS8 1TL, United Kingdom.

[e]University Libre de Bruxelles, B-1050 Brussels, Belgium.

[f]University of California Irvine, Irvine, CA 92697, USA.

[g]University of California Santa Cruz, Santa Cruz, CA 95064, USA.

[h]Cornell University, Ithaca, NY 14853, USA.

[i]University of Cyprus, Nicosia CY-1678, Cyprus.

[j]University College Dublin, Dublin 4, Ireland.

[k]University of Edinburgh, Edinburgh EH9 3JZ, United Kingdom.

[l]University of Heidelberg, D-69120 Heidelberg, Germany.

[m]Universidad Iberoamericana, Mexico D.F., Mexico.

[n]University of Manchester, Manchester M13 9PL, United Kingdom.

[o]Nagasaki Institute of Applied Science, Nagasaki, Japan.

[p]University de Oviedo, E-33007 Oviedo, Spain.

[q]Queen Mary, University of London, London E1 4NS, England.

[r]Texas Tech University, Lubbock, TX 79409, USA.

[s]IFIC (CSIC–Universitat de Valencia), 46071 Valencia, Spain.

[1] J. J. Aubert *et al.*, Phys. Rev. Lett. **33**, 1404 (1974).

[2] J. E. Augustin *et al.*, Phys. Rev. Lett. **33**, 1406 (1974).

[3] M. Gell-Mann and A. Pais, Phys. Rev. **97**, 1387 (1955).

[4] C. Albajar *et al.* (UA1 Collaboration), Phys. Lett. B **186**, 247 (1987).

[5] H. Albrecht *et al.* (ARGUS Collaboration), Phys. Lett. B **192**, 245 (1987).

[6] A. Abulencia *et al.* (CDF Collaboration), Phys. Rev. Lett. **97**, 242003 (2006).

[7] B. Aubert *et al.* (*BABAR* Collaboration), Phys. Rev. Lett. **98**, 211802 (2007).

[8] M. Starič *et al.* (Belle Collaboration), Phys. Rev. Lett. **98**, 211803 (2007).

[9] After our paper was submitted, *BABAR* submitted a result confirming the Belle evidence, arXiv:0712.2249.

[10] L. M. Zhang *et al.* (Belle Collaboration), Phys. Rev. Lett. **96**, 151801 (2006).

[11] M. Gronau and J. L. Rosner, Phys. Lett. B **500**, 247 (2001).

[12] A. F. Falk *et al.*, Phys. Rev. D **69**, 114021 (2004).

[13] E. Golowich and A. A. Petrov, Phys. Lett. B **625**, 53 (2005).

[14] G. Burdman and I. Shipsey, Annu. Rev. Nucl. Sci. **53**, 431 (2003). See section 2.3.

[15] E. Golowich, S. Pakvasa, and A. A. Petrov, Phys. Rev. Lett. **98**, 181801 (2007).

[16] E. Golowich, J. Hewett, S. Pakvasa, and A. A. Petrov, Phys. Rev. D **76**, 095009 (2007).

[17] G. Blaylock *et al.*, Phys. Lett. B **355**, 555 (1995).

[18] R. Godang *et al.* (CLEO Collaboration), Phys. Rev. Lett. **84**, 5038 (2000).

[19] D. Acosta *et al.* (CDF Collaboration), Phys. Rev. D **71**, 032001 (2005).

[20] A. Abulencia *et al.* (CDF Collaboration), Phys. Rev. D **74**, 031109(R) (2006).

[21] W.-M. Yao *et al.* (Particle Data Group), J. Phys. G **33**, 1 (2006).